Released Plasmonic Electric Field of Ultrathin Tetrahedral-Amorphous-Carbon Films Coated Ag Nanoparticles for SERS

Fanxin Liu[1,2], Chaojun Tang[2], Peng Zhan[1], Zhuo Chen[1], Hongtao Ma[3] & Zhenlin Wang[1]

[1]National Laboratory of Solid State Microstructures and School of Physics, Nanjing University, Nanjing 210093, PR China, [2]Department of Applied Physics, Zhejiang University of Technology, Xiaoheshan, Hangzhou 310023, PR China, [3]SAE Magnetics (HK) Ltd (TDK), Dongguan 523087, PR China.

We have demonstrated the plasmonic characteristics of an ultrathin tetrahedral amorphous carbon (ta-C) film coated with Ag nanoparticles. The simulation result shows that, under resonant and non-resonant excitations, the strongest plasmonic electric field of 1 nm ta-C coated Ag nanoparticle is not trapped within the ta-C layer but is released to its outside surface, while leaving the weaker electric field inside ta-C layer. Moreover, this outside plasmonic field shows higher intensity than that of uncoated Ag nanoparticle, which is closely dependent on the excitation wavelength and size of Ag particles. These observations are supported by the SERS measurements. We expect that the ability for ultrathin ta-C coated Ag nanoparticles as the SERS substrates to detect low concentrations of target biomolecules opens the door to the applications where it can be used as a detection tool for integrated, on-chip devices.

T he detection of biomolecules by optical methods is of much interest in the fields of pollutants, diseases diagnostics, and pharmaceuticals[1–6]. Now Raman technique has been extensively employed. As compared with other techniques, such as IR, Raman detection can provide rich fingerprint information as well as quantitative and qualitative information of molecules[1]. In addition, Raman detection will not be interfered by the presence of water commonly existing in all biological samples[5]. However, conventional Raman technique usually lacks sufficient sensitivity for its use as a readout method in low concentration bio-analysis, which largely limits its applications[7].

Now plasmonics is a flourishing field of science and technology that exploits the unique optical properties of metal nanostructures to manipulate light at the nanoscale[8,9]. Metal nanostructures derive novel optical properties from their ability to support the excitation of surface plasmon (SP)[8]. By properly engineering the morphology and size of metallic nanostructures, light can be concentrated and significantly enhanced and the localized electric fields are formed at specific locations of the nanostructure surfaces[9]. This enhanced electric field can improve Raman signals, even at single molecular level, named as surface enhanced Raman scattering (SERS)[10,11].

For the study about SERS-active substrates, dielectric layer coated metallic nanostructures are of much interest due to the following reasons[12–19]. Firstly, a dielectric layer can keep the nanoparticles from agglomerating, separating them from a direct contact[12,13]. Secondly, dielectric layers can be functionalized to fulfill special requirements, for example, chemical stability, especially for Ag[13,14,16,17,20]. Though Ag is of special significance in optical applications due to its strong SP resonance and a broader frequency range compared to other plasmonic metal elements, it is susceptible to oxidation under ambient conditions and accordingly has a weaken SP resonance[19]. The covering of dielectric layer can improve the chemical stability of Ag nanostructures as well as preserve the features of their SP resonances. Among a variety of the dielectric layers, the Al_2O_3 and SiO_2 films are extensively investigated[12,13,16]. Some groups have reported very important results[12,16]. For instance, Van Duyne et al. have studied the ultrathin Al_2O_3 coated Ag nanosphere arrays for the improved chemical stability as well as good SERS activity[16]. Furthermore, Tian et al. have described a new technique called shell-isolated nanoparticle-enhanced Raman spectroscopy that harnesses the enhancing properties of Au nanoparticles with an ultrathin SiO_2 shell ($\sim$4 nm) as smart dust, which may include a wider range of applications, such as to probe surface composition[12]. These important researches will help to realize the practical applications for SERS.
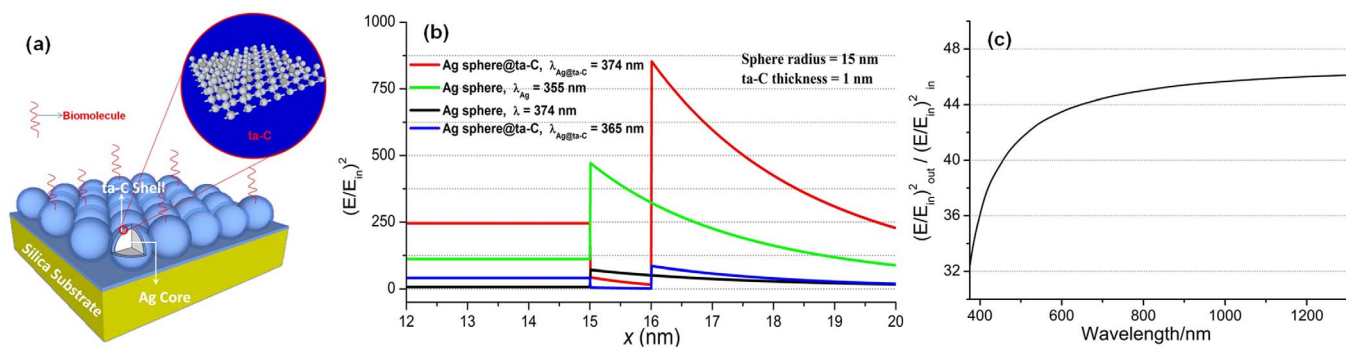
Figure 1 | (a) Schematic of ultrathin ta-C films coated Ag nanoparticles for SERS biomolecule detection. (b) Plasmonic electric field intensity $(E/E_{in})^2$ plotted for the 30 nm-Ag/1 nm-ta-C and Ag nanosphere at their respective SP resonant and non-resonant excitations. (c) The change trend of the ratio of $(E/E_{in})^2_{out}$ at the interface of ta-C/air to the $(E/E_{in})^2_{in}$ at the interface of Ag/ta-C as a function of excitation wavelengths from 375 to 1300 nm for the 30 nm-Ag/1 nm-ta-C.

Usually, a common drawback in thicker dielectric layers coated metallic hybrids is that the highest plasmonic electric fields are tightly trapped inside the dielectric layer, thus yielding a relative lower SERS sensitivity. If the thickness of dielectric layer becomes thinner, the plasmonic electric field intensity located at the outer surface of dielectric layer will have a further increase. Therefore, for the SERS application, how to reduce the thickness of dielectric layer to be ultrathin and make the highest electric field of metal/dielectric hybrid Ag nanostructure to be released to the outside of dielectric layer as well as keep good chemical stability is of scientific and technological importance. In a recently reported work, a theoretical study of ultrathin SiO_2 film coated Ag spheres dimer for SERS showed that the coated dimer could give a higher SERS enhancement factor compared to uncoated dimer[13]. This seems to be a little counter-intuitive, according to the common knowledge that a dielectric layer would trap and decay the plasmonic electric fields.

Here, we present a new ultrathin dielectric of tetrahedral amorphous carbon (ta-C) film. A ta-C film is an amorphous carbon material which contains a 90% content of sp^3 (diamond structure) bonding[23–26], which is dense and pinhole-free even with the thickness up to 1 nm. Owing to the relatively small size of the carbon atom and the short interatomic distance, the structure of ta-C film could be much superior as compared with the Al_2O_3 and SiO_2 films, especially in the case of ultrathin thickness. Thus we suppose that the ta-C film may be a good candidate as the ultrathin dielectric layer. In our previous report, we have experimentally demonstrated that the Ag nanoprism arrays coated by an extremely thin ta-C layer (for example, 1-nm-thickness) show a higher enhancement of Raman signals than the uncoated ones, as well as show Ag oxygen-free, which is quite different from conventional understand that a thick dielectric coating layer might lead to the electric field decay exponentially away from the metallic nanoparticle's surface[17]. In this letter, using classic Mie theory and quasi-static approximation, we clearly demonstrate the plasmonic characteristic of 1 nm ta-C coated Ag nanosphere under the resonant and non-resonant excitations for different Ag nanosphere sizes to show that the highest plasmonic electric field of 1 nm ta-C coated Ag nanoparticle is not trapped within the ta-C layer but is released to its outside surface, while leaving the weaker electric field inside ta-C layer. To make a proof-of-principle investigation, we have performed the experimental illustration by SERS in 1 nm ta-C coated Ag nanospheres. Finally, as an example, we have also tried to utilize this novel SERS substrate for a direct detection of the melamine mixed in milk. We expect that our study can open the door to the applications where this novel SERS substrate can be used as a detection tool for integrated, on-chip devices.

Results
Our design is shown schematically in Figure 1a. In order to confirm the speculation of releasing electric field by an ultrathin dielectric coating layer, firstly we have calculated electric field intensity $(E/E_{in})^2$ of a single Ag nanosphere coated with 1 nm ta-C film at its SP resonance of 374 nm by Mie theory[21], as shown by red line in Figure 1b. In the calculation, Ag nanosphere is assumed to have a diameter of 30 nm which is consistent with the size of Ag nanoparticle fabricated in the experiment presented later, and the relative permittivity of Ag is taken from experimental data[22]. The ta-C refractive index thickness with 1 nm is measured to be ~2.4 in the spectrum range from 300 to 1300 nm by the Woollam (M2000 DI with focus probes). By performing the measurements with the different angles, it is found that the refractive index of ta-C is almost unchanged, which indicates that 1 nm ta-C could be thought to be homogeneous. If the thickness of ta-C is over 20 nm, its refractive index will be increased to be ~2.66 which is very close to that of diamond. For the simplicity in calculation, only the $(E/E_{in})^2$ on the equatorial line for the sphere model is shown and other locations biased with center is not shown due to similar results. It is very interesting to be found that, not like a thicker dielectric coating which has been well studied previously, the biggest $(E/E_{in})^2$ is not at the Ag/ta-C but is at the ta-C/air interface which can be understood as the releasing here. In contrast, the $(E/E_{in})^2$ in the ta-C shell has a rapid decrease and approaches to be zero from the interface of Ag/ta-C, and then the $(E/E_{in})^2$ abruptly increases at the ta-C/air. In order to further confirm this rapid change of electric field intensity in the ta-C shell, we have done the quasi-static approximation analysis to confirm this, shown in Supporting Information. Mention that, $(E/E_{in})^2$ is not completely zero in the ta-C film, and this also can be seen in our numerical results in Figure 1b. In fact, the smallest value of $(E/E_{in})^2$ in the ta-C film is about 18, and the largest value is about 45.

Secondly, at its non-resonance excitation of 365 nm, the $(E/E_{in})^2$ of 30 nm Ag nanosphere coated with 1 nm ta-C film is also calculated, as shown by blue line in Figure 1b. The electric field distribution in the ta-C and out of the ta-C is similar to that at the resonant excitation of 374 nm. Furthermore, we have calculated the ratio of $(E/E_{in})^2$ at the ta-C/air to that at the Ag/ta-C interface upon the wavelength range from 400 to 1300 nm for the 30 nm Ag nanosphere coated with 1 nm ta-C film, shown in Figure 1c. The results show that the $(E/E_{in})^2$ at the interface of ta-C/air is always larger than that at the interface of Ag/ta-C. In addition, the electric field distribution of the 1 nm ta-C coated Ag nanosphere diameter with a bigger size of 170 nm is also calculated both at the resonant wavelength of 514 nm, and at the non-resonant wavelengths of 480 nm (blue shift) and 600 nm (red shift), shown in Figure S2. The results also show that the biggest $(E/E_{in})^2$ is not at the interface of Ag/ta-C but is released to the interface of ta-C/air.

Furthermore, in order to clarify the influence of ta-C thickness on this releasing, we have calculated the $(E/E_{in})^2$ on the equatorial line for the ta-C coated Ag nanosphere with the thickness varying from 1
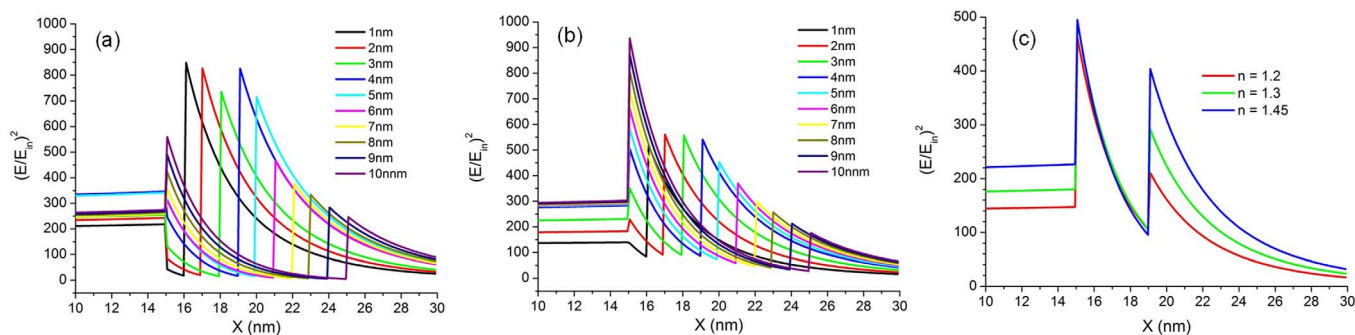
Figure 2 | $(E/E_{in})^2$ on the equatorial line distribution of 30 nm Ag sphere coated with ta-C films (a) and Al_2O_3 films (b) thickness varying from 1 to 10 nm at their respective resonances. (c) $(E/E_{in})^2$ distribution of 30 nm Ag sphere coated with 4 nm dielectric films with the refractive index varying from 1.45 to 1.2.

to 10 nm at their respective resonance wavelengths, shown in Figure 2a. The result shows that the critical thickness of ta-C for the releasing is $7 \sim 8$ nm, and the $(E/E_{in})^2$ at the interface of ta-C/air will become smaller than that at the interface of Ag/ta-C when the ta-C thickness is over ~8 nm. Typical electric field distribution of the ta-C coated Ag nanosphere is shown in Figure S3. As compared to conventional dielectric layers such as Al_2O_3 or SiO_2 films, our new ta-C ultrathin film has a higher refractive index. As an example, the $(E/E_{in})^2$ for the Al_2O_3 coated Ag nanosphere with the thickness varying from 1 to 10 nm at their respective resonance wavelengths, as shown in Figure 2b. In the calculation, the refractive index of Al_2O_3 film assumes to be 1.6 by considering the ultrathin thickness, which is smaller than that of ta-C film. Similar to ta-C films, $(E/E_{in})^2_{out}/(E/E_{in})^2_{in}$ is larger than 1 when the thickness of Al_2O_3 film is thinner than $4 \sim 5$ nm. If further decreasing the refractive index from 1.45 (such as SiO_2) to 1.2, one can expect that the critical thickness would become much thinner, as shown in Figure 2c. More importantly, Figure 2a&b also indicates that, under the same coating thickness, $(E/E_{in})^2$ at the outside surface of dielectric layer with higher refractive index is higher than that with smaller refractive index, which is due to a better confinement of light for the higher refractive index dielectric materials. From this viewpoint, the ta-C could be better than the Al_2O_3 or SiO_2 as a dielectric protective layer.

Considering the characteristics of plasmonic dielectric/metal hybrid structure in which the plasmonic electric field is the maximum at the interface of metal and dielectric and decays exponentially in the directions perpendicular to the interface, we mainly consider 1 nm ta-C as ultrathin dielectric layer for the better SERS performance, combining with its mechanical properties in this letter[17]. It is note here that the electric field for the 4 nm ta-C higher than that for the 3 nm ta-C shown in Figure 2(a) is induced by the change trend of the imaginary part of Ag relative permittivity (ε) as a function of wavelength (experimental data by Johnson et al, Figure S4 in black line), which will be presented in the following.

In practical applications in SERS, the comparison between this released electric field on the outside surface of dielectric and the electric field for the Ag nanostructure without coating is also very important. As shown in Figure 1b, the highest $(E/E_{in})^2$ of a bare 30 nm Ag nanosphere at its SP resonance of 355 nm is lower than that of 1 nm ta-C coated Ag nanosphere at the resonance of 374 nm. In contrast, $(E/E_{in})^2$ of uncoated Ag at resonant excitation of 355 nm is higher than that 1 nm ta-C coated Ag at the non-resonant excitation of 365 nm. According to the change trend of the imaginary part of Ag relative permittivity (ε) as a function of wavelength (experimental data by Johnson et al, Figure S4 in black line), the imaginary part of ε has a decrease from the 340 to 382 nm so that a red shift from 355 to 375 nm under 1 nm ta-C coating will lead to a lower loss at their respective resonances. Obviously, Drude model (Figure S4 in red line) for the Ag relative permittivity is not suitable here. If the size of Ag nanostructure becomes larger and its resonance red-shifts to 785 nm, additional ultrathin dielectric coating may lead to a larger loss for the electric field intensity, which is confirmed by Van Duyne's group using ultrathin Al_2O_3 coated Ag nanosphere arrays[16]. Thus, the electric field enhancement of 1 nm ta-C coated Ag nanostructures as compared to the uncoated Ag is related to the excitation wavelength and size of Ag particles.

In the experiment, the Ag near-spherical nanoparticles are firstly fabricated using a gas phase deposition of performed clusters onto a fused quartz glass substrate as described previously and the deposition time is 10 min[27]. Figure 3a shows a typical SEM image which
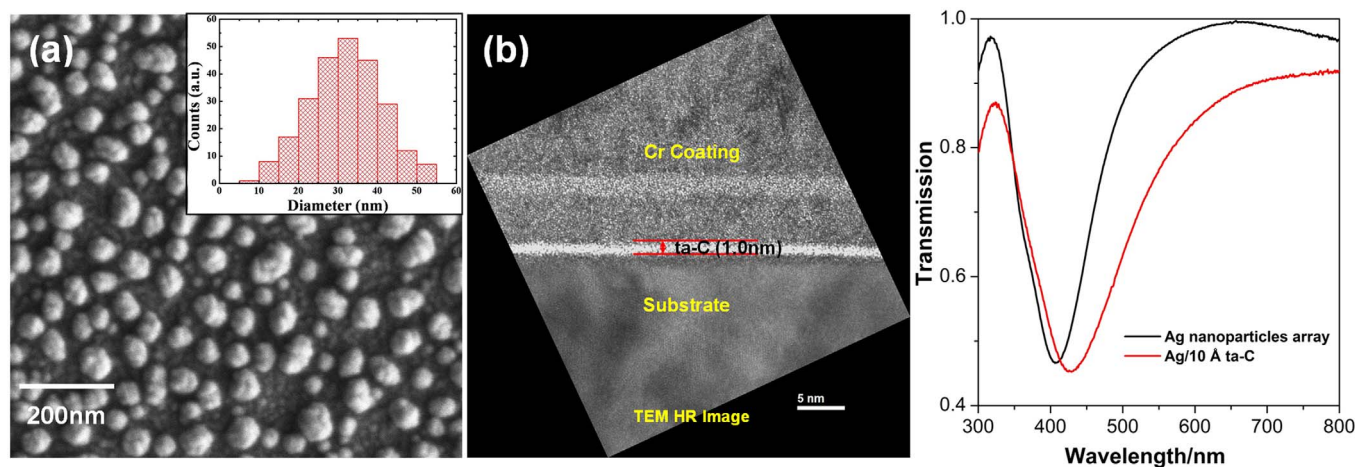
Figure 3 | (a) SEM image of the Ag nanoparticles film. (b) TEM cross section of ta-C films deposited on the monitored Si substrate. (c) Transmittance spectra of the 1 nm ta-C film coated Ag nanoparticles and uncoated Ag nanoparticles substrates.

shows that the Ag nanoparticles are isolated from each other and cover the substrate with a sub-monolayer. The Ag nanoparticles have no aggregation of Ag nanoparticles on the quartz glass substrate. The size distribution of the particles is measured and shown in the inset in Figure 3a, which fits a lognormal distribution with a most frequent apparent diameter of ~30 nm. Here the average size and shape of fabricated Ag particles are approximated as the Ag nanosphere described in above model. Then the substrate is coated with an ultra-thin ta-C film with a thickness of 1 nm (here denoted as Ag/1 nm-ta-C).

Figure 3b shows the high resolution transmission electron microscope (HR-TEM) cross-section analysis of ta-C film with the thickness of 1 nm deposited in our monitored Si substrate, and the result shows that the thickness of ta-C films is well controlled. The TEM image also shows that the prepared ta-C films have good uniformity. The plasmonic characteristics of Ag/1 nm-ta-C substrates, which are of primary importance to the investigation of the SERS, were performed by measuring the transmission spectra using a UV–Visible spectrophotometer under normal incidence of an unpolarized light, as shown in Figure 3c. For both Ag/1 nm-ta-C and uncoated Ag nanoparticles, the transmittance spectra have a broad-band dip, which is due to the excitation of a dipole SP resonance. As compared to the uncoated Ag, the dipole SP resonance of Ag/1 nm-ta-C shows a small red shift of 15 nm due to an ultrathin dielectric coating, and is centered at *ca.* 417 nm, which has a partial overlap with the excitation wavelength of 514 nm used in the Raman testing. This shift is very small as compared to peak width, though the ta-C has a high refractive index value[17]. The excitation of this localized surface plasmon resonance will lead to a locally enhanced electromagnetic field which is responsible for the SERS presented later.

In addition, in order to confirm that the prepared ta-C films thickness with 1 nm are pinhole-free and dense, which is very important to our design in which the 1 nm ta-C is thought to be pinhole-free, we have performed oxalic acid corrosion test based on the industrial standard (Figure S5). The results show that the ta-C film becomes pinhole-free by increasing its thickness to be ~1 nm or above. In our previous paper[17,18], we have also demonstrated that a 1 nm or thicker ta-C film can efficiently protect the oxygen-free Ag in air. Thus, our ta-C films thickness with 1 nm can be thought to be dense and pin-hole-free. Combining the pinhole-free characteristic of the prepared ta-C film and our theoretical model, it suggests that the Ag/1 nm-ta-C substrate could give a good SERS activity.

To support our theoretical model, the Raman testing is performed and the measured SERS spectra of the R6G molecules adsorbed on both the Ag/1 nm-ta-C film and the uncoated Ag nanoparticles film are shown in Figure 4. It is noted here that it is difficult to direct comparison for the inner and outer electric field of 1 nm ta-C coated Ag nanoparticles, due to the impossible contact of probe molecules to the inner electric field in ta-C. Here we only compared the electric field for the coated and uncoated Ag nanosphere at the same excitation wavelength of 514 nm for the confirmation by SERS testing. During the experiment, an aqueous solution of Rhodamine 6G (R6G) 10^{-4} M was used. To allow the molecule adsorption, the substrates were first maintained in R6G solution for 24 h, then taken out and rinsed thoroughly with ethanol, and finally dried with nitrogen gas. It is noted here that a long incubation time and rinse process can ensure that the coverage of the R6G molecule single layer on both the Ag and ta-C surface is nearly the same. The spectra of R6G on the Ag/1 nm-ta-C and Ag nanoparticles alone are much the same as that reported previously, which has been extensively analyzed, thus its spectral assignment will not be discussed here[28]. In Figure 4, the result shows that the Raman signal intensity on the Ag/1 nm-ta-C substrate is higher than that on uncoated Ag nanoparticles substrate. Furthermore, by the calculation of electric field intensity of coated and uncoated Ag nanoparticles at 514 nm according to experimental data of Ag dielectric constant (Figure S6), the result also indicates
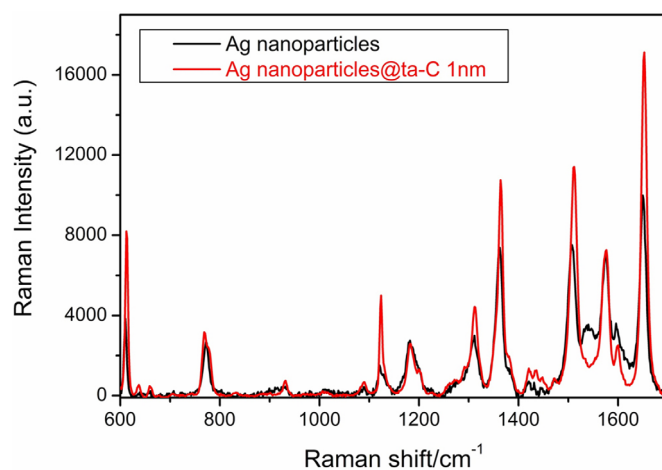

Figure 4 | SERS spectra of 10^{-4} M R6G molecules absorbed on the Ag nanoparticles substrate (black line) and 1 nm ta-C film coated Ag nanoparticles substrate (red line).

that the electric field intensity of 30 nm-Ag/1 nm-ta-C is a little higher than that of uncoated 30 nm Ag, which is consistent with the experimental results. In addition, we have also measured the Raman spectra on five different locations in same conditions for coated and uncoated substrates, and the results indicated that the probed molecule Raman intensities were very similar (data not shown here), which was due to the bigger laser spot size and relatively smaller and uniform Ag nanoparticles in experiment.

Discussion

When the ta-C dielectric layer becomes extremely ultrathin, a dense ta-C coating will release, rather than trap the strongest plasmonic electric field, which is better for the Raman signal improvement on the ta-C film coated Ag nanoparticles. Based on these experimental and numerical simulations results, we proposed a model to explain this fantastic characteristic. This could be explained in the following physical picture possibly. Since the dielectric layer becomes ultrathin, it cannot confine the electric field well inside the dielectric and more photons can spill over from the inside of the dielectric layer to its outside surface, and thus forming a higher electric field focused on the interface of dielectric/air, which can be understood as photon tunneling. However, if the ta-C becomes thicker than the critical thickness, the photon tunneling process will be largely decreased, and then the strongest plasmonic electric field will still focus on the interface of Ag/dielectric. Our strategy of releasing plasmonic electric field could be very useful to many photonic processes happened near it.

Finally, using the 1 nm ta-C coated Ag nanoparticles as a SERS substrate, industrial melamine in milk is tried to be analyzed as an example in the application, shown in Figure 5. Because of its high nitrogen content (66%) and low cost, the melamine has been illegally added to food products in order to increase apparent protein content[2]. During the SERS detection, a milk solution of melamine at 2.5 mg/L (China National Standard) was used. The SERS spectra were acquired using a Renishaw Invia Raman microscope system with the laser operating at a wavelength of 514 nm with 0.05 mW laser output power, 10 s collection time, and a 50X magnification objective. In the testing, the glass substrate was used for conventional Raman detection. In addition, the Raman spectrum of only milk on the SERS substrate was also performed for better comparison (Figure S7), which indicated that there was no any Raman signal. The spectra feature of melamine on the Ag/1 nm-ta-C shows some difference from the previous report[29]. The difference with the normal Raman spectrum of melamine in aqueous solution may be ascribed to the bonding connection between the melamine molecule and milk.
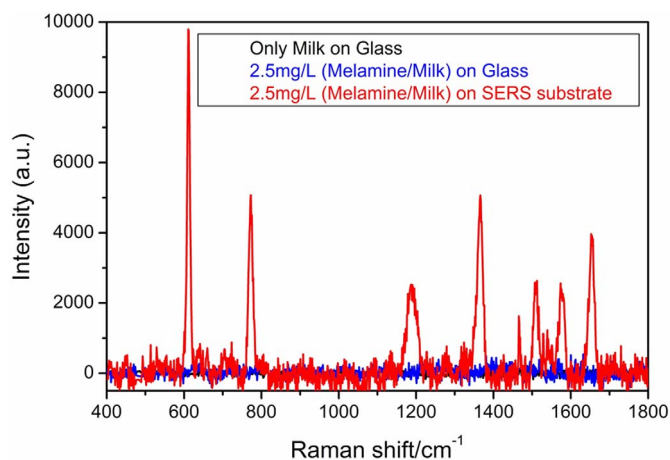
Figure 5 | Raman spectra of melamine molecules mixed with milk (2.5 mg/L) absorbed on the 1 nm ta-C coated Ag nanoparticle SERS substrate (red line), and on the glass (blue line). Raman spectrum of only milk on glass is for reference (black line).

These results show that the melamine in milk solution under the china national standard can be easily detected by our proposed substrate, while conventional Raman is incapable of detecting it. Thus we expect that the ability for an ultrathin ta-C coated Ag nanoparticles SERS substrate to detect low concentrations of target biomolecules could open the door to the applications where it can be used as a detection tool for integrated, on-chip devices.

Methods

Silver nanoparticle fabrication. Ag nanoparticles were produced in a magnetron cluster source. During the fabrication, the 200 sccm argon was introduced into the liquid nitrogen cooled aggregation tube to maintain a stable gas flow with a pressure of 180 Pa. The clusters were extracted from the aggregation tube into high vacuum through a differential pumping system. Performed clusters were deposited at low kinetic energy (<0.1 ev/atom) onto the surfaces of substrates maintained at room temperature in a high vacuum chamber. During deposition, the pressure of the deposition chamber was ~10^{-5} Torr. The deposition rate was monitored by a quartz crystal microbalance and controlled at about 0.5 Å/s by a discharge power of 90 W. The prepared samples were thermally annealed at 180°C for 10 min in a vacuum.

Ta-C deposition. The ta-C film was fabricated by using a multifilm deposition system with a combination of a *FCVA* (filtered cathodic vacuum arc) gun. The deposition rate monitored by an ellipsometer was ~0.5 Å per second.

Characterizations. The morphology of Ag films was characterized with a scanning electron microscope (SEM, Hitachi, S-4800) operated at an accelerating voltage 2 KV and an average working distance of 8.2 mm.

SERS testing. An aqueous solution of Rhodamine 6G (R6G) 10^{-4} M was used. To allow the molecule adsorption, the prepared substrates were first maintained in R6G solution for 24 h, then taken out and rinsed thoroughly with ethanol, and finally dried with nitrogen gas. SERS spectra were acquired using a Renishaw Invia Raman microscope system with the laser operating at a wavelength of 514 nm with 0.2 mW laser output, a 10 s collection time, and a 50X magnification objective.

1. Cui, Y., Ren, B., Yao, J. L., Gu, R. A. & Tian, Z. Q. Synthesis of Ag$_{core}$Au$_{shell}$ Bimetallic nanoparticles for immunoassay based on surface-enhanced Raman spectroscopy. *J. Phys. Chem. B* **110**, 4002–4006 (2006).
2. Wei, F. *et al.* Rapid detection of melamine in whole milk mediated by unmodified gold nanoparticles. *Appl. Phys. Lett.* **96**, 133702 (2010).
3. Verellen, N. *et al.* Plasmon Line Shaping Using Nanocrosses for High Sensitivity Localized Surface Plasmon Resonance Sensing. *Nano Lett.* **11**, 391–397 (2011).
4. Liu, N., Tang, M. L., Hentschel, M., Giessen, H. & Alivisatos1, A. P. Nanoantenna-enhanced gas sensing in a single tailored nanofocus. *Nat. Mater.* **10**, 631–636 (2011).
5. Li, M. *et al.* Detection of Adenosine Triphosphate with an Aptamer Biosensor Based on Surface-Enhanced Raman Scattering. *Anal. Chem.* **84**, 2837–2842 (2012).
6. Xu, T. T. *et al.* Ordered silicon nanocones arrays for label-free DNA quantitative analysis by surface-enhanced Raman spectroscopy. *Appl. Phys. Lett.* **99**, 153116–1 (2011).
7. Doering, W. E., Piotti, M. E., Natan, M. J. & Freeman, R. G. SERS as a foundation for nanoscale, optically detected biological Labels. *Adv. Mater.* **19**, 3100–3108 (2007).
8. Barnes, W. L., Dereux, A. & Ebbesen, T. W. Surface Plasmon Subwavelength Optics. *Nature* **424**, 824–830 (2003).
9. Schuller, J. A. *et al.* Plasmonics for Extreme Light Concentration and Manipulation. *Nat. Mater.* **9**, 193–204 (2010).
10. Nie, S. M. & Emory, S. R. Probing Single Molecules and Single Nanoparticles by Surface-Enhanced Raman Scattering. *Science* **275**, 1102–1106 (1997).
11. Xu, H. X., Bjerneld, E. J., Kall, M. & Borjesson, L. Spectroscopy of Single Molecules by Surface Enhanced Raman Scattering. *Phys, Rev. Lett.* **83**, 4357–4360 (1999).
12. Li, J. F. *et al.* Shell–Isolated Nanoparticles–Enhanced Raman Spectroscopy. *Nature* **464**, 392–395 (2010).
13. Xu, H. X. Theoretical Study of Coated Spherical Metallic Nanoparticles for Single–Molecule Surface-Enhanced Spectroscopy. *Appl. Phys. Lett.* **85**, 5980–4982 (2004).
14. Uzayisenga, V. *et al.* Synthesis, Characterization, and 3D-FDTD Simulation of Ag@SiO2 Nanoparticles for Shell-Isolated Nanoparticle-Enhanced Raman Spectroscopy. *Langmuir* **28**, 9140–9146 (2012).
15. Sun, Z. H., Bao, Z. H., Fang, C. H. & Wang, J. F. Formation of Different Gold Nanocrystal Core−Resin Shell Structures through the Control of the Core Assembly and Shell Polymerization. *Langmuir* **28**, 9082–9092 (2012).
16. Zhang, X. Y., Zhao, J., Whitney, A. V., Elam, J. W. & Van Duyne, R. P. Ultrastable Substrates for Surface-Enhanced Raman Spectroscopy: Al2O3 Overlayers Fabricated by Atomic Layer Deposition Yield Improved Anthrax Biomarker Detection. *J. Am. Chem. Soc.* **128**, 10304–10309 (2006).
17. Liu, F. X., Cao, Z. S., Tang, C. J., Chen, L. & Wang, Z. L. Ultrathin Diamond-like carbon film coated silver nanoparticles based substrates for surface-enhanced Raman spectroscopy. *ACS Nano* **4**, 2643–2648 (2010).
18. Liu, F. X., Tang, C. J., Pan, J., Cao, Z. S. & Wang, Z. L. A strategy for maximum fluorescence enhancement based on ta-C coated metal substrates. *J. Phys. Chem. C* **114**, 9871–9875 (2010).
19. Feng, J. J. *et al.* Novel Au–Ag Hybrid Device for Electrochemical SERR Spectroscopy in a Wide Potential and Spectral Range. *Nano Lett.* **9**, 298–303 (2009).
20. Im, H., Lindquist, N. C., Lesuffleur, A. & Oh, S. H. Atomic Layer Deposition of Dielectric Overlayers for Enhancing the Optical Properties and Chemical Stability of Plasmonic Nanoholes. *ACS Nano* **4**, 947–954 (2010).
21. Bohren, C. F. & Huffman, D. R. Absorption and Scattering of Light by Small Particles. (Wiley, New York, 1983).
22. Johnson, P. B. & Christy, R. W. Optical Constants of the Novel Metals. *Phys. Rev. B* **6**, 4370–4379 (1972).
23. Robertson, J. Diamond-like Amorphous Carbon. *Mater. Sci. Eng. R* **37**, 129–281 (2002).
24. Liu, F. X., Yao, K. L. & Liu, Z. L. Substrate bias effect on structure of ta-C films by Raman spectroscopy. *Diamond Relat. Mater.* **16**, 1746–1751 (2007).
25. Dearnaley, G. & Arps, H. J. Biomedical Applications of Diamond-like Carbon (DLC) Coatings: A Review. *Surf. Coat. Technol.* **200**, 2518–2524 (2005).
26. Liu, F. X. & Wang, Z. L. Thickness Dependence of the Structure of Diamond-like Carbon Films. *Surf. Coat. Technol.* **203**, 1829–1832 (2009).
27. Xu, C. H. *et al.* Enhanced Thermal Stability of Monodispersed Silver Cluster Arrays Assembled on Block Copolymer Scaffolds. *Nanotechnology* **21**, 195304: 1–6 (2010).
28. Baia, M., Baia, L., Astilean, S. & Popp, J. Surface-Enhanced Raman Scattering Efficiency of Truncated Tetrahedral Ag Nanoparticle Arrays Mediated by Electromagnetic Coupling. *Appl. Phys. Lett.* **88**, 143121(2006).
29. Li, J. M. *et al.* Detecting Trace Melamine in Solution by SERS Using Ag Nanoparticle Coated Poly (styrene-co-acrylic acid) Nanospheres as Novel Active Substrates. *Langmuir* **27**, 14539–14544 (2011).

Author contributions

F.L. and Z.W. conceived and designed the experiments, and analyzed the results. F.L., H.M. and P.Z. performed the experiments. C.T. and Z.C. performed the numerical simulation. Manuscript was written by F.L. and Z.W.

Additional information